

A method of vehicle motion prediction and collision risk assessment with a simulated vehicular cyber physical system



Chaozhong Wu ^{a,b,*}, Liqun Peng ^{a,b}, Zhen Huang ^c, Ming Zhong ^{a,b}, Duanfeng Chu ^{a,b}

^a Intelligent Transport Systems Research Center, Wuhan University of Technology, 1040 Heping Avenue, Wuhan, Hubei 430063, China

^b Engineering Research Center for Transportation Safety, Ministry of Education, 1040 Heping Avenue, Wuhan, Hubei 430063, China

^c School of Automation, Wuhan University of Technology, 205 Luoshi Road, Wuhan, Hubei 430070, China

ARTICLE INFO

Article history:

Received 8 October 2013

Received in revised form 11 July 2014

Accepted 11 July 2014

Available online 2 September 2014

Keywords:

Collision avoidance

Vehicular cyber physical system

Driver behavior

Vehicle path prediction

Risk assessment

ABSTRACT

Vehicular cyber physical system (VCPS) can comprehensively acquire road traffic safety related information, and provide drivers with early warning or driving assistance in emergency, in order to assist them avoid vehicle crash in the driving process. Literature review shows that previous studies mainly rely on observed vehicle motion/location data for assessing vehicle collision risk, where predicted vehicle motion/location, driver behavior and road geometry (e.g., curvature) are rarely considered. In this study, based on the simulated VCPS, a collision avoidance system that can explicitly consider the above issues is designed and presented in detail. Within the proposed collision avoidance system, an assessment method, which can predict collision risk by comprehensively considering vehicles motion/location, driver behavior and road geometry information from the VCPS, is developed. Firstly, the short-term motion of the objective vehicle and surrounding vehicles are predicted based on the Kalman Filter (KF) algorithm and the vehicle motion model. Furthermore, the proposed method that can explicitly take driver behavior and road curvature into account is used to predict vehicle location and calculate the traveled distance among vehicles in real-time. Then, the predicted vehicle gaps are compared with a safe distance threshold and the vehicle collision risk is predicted. Finally, the accuracy of the proposed collision risk assessment method is examined with a receiver operating characteristic (ROC) curve analysis over a section of curved road. Simulation results show that the proposed method is effective for detecting collision risk and providing accurate warnings in a timely fashion.

© 2014 Elsevier Ltd. All rights reserved.

1. Introduction

Vehicle collision avoidance system has been one of popular research topics in the field of intelligent transportation system (ITS). It can detect accident risk and promptly warn the driver, in order to avoid collision. According to National Highway Traffic Safety Administration (NHTSA), 79% of rear-end accidents were due to driver distraction, and the accident rate can be reduced to 60% if drivers pay attention to the risk half a second early. Research at Benz Company also shows that if driver can detect the accident risk one or two seconds early and take correct operation, most of traffic accidents can be avoided (Liu et al., 2010). Thus, a real-time and accurate prediction of collision risk is important to a desired vehicle collision warning system.

* Corresponding author at: Intelligent Transport Systems Research Center, Wuhan University of Technology, 1040 Heping Avenue, Wuhan, Hubei 430063, China.

Previous collision avoidance systems (CAS) assess driving safety by measuring the current time-to-collision (TTC) or headway time (HT). Vehicle motion and road geometry are mostly ignored. Obviously, these factors should be considered in a CAS, if it is supposed to provide more effective warnings and assistance to driver in a complex traffic and road environment. The challenge of developing the next generation CAS is to reconstruct the vehicle's environment in order to timely provide warnings and prevent collisions in the longitudinal, rear and lateral dimension and therefore the above must be considered.

In this study, a vehicular cyber physical system is developed within a simulation software – CARSIM, which can acquire vehicle motion/location, driver behavior and road geometry every half second. Coupled with a collision risk assessment method, it can predict the motion of objective vehicle and adjacent obstacles based on a Kalman Filter (KF) algorithm and assess collision risk in real-time. The proposed system can be used to predict vehicle motion and location in dynamic, including vehicle path, speed, traveled distance and assess collision risk based on data collected through the virtual sensors. It should be noted that the simulated VCPS is constructed based on a set of virtual sensors, which are very common and therefore the proposed system can be easily implemented in the field.

The paper is organized as follows: Section 2 presents a brief overview to research about Application of VCPS on vehicle crash avoidance system, vehicle motion model and driver behavior decision model. Section 3 introduces the general architecture of the proposed VCPS-based collision avoidance system. Section 4 describes the proposed collision risk assessment method, including a road geometry model, an improved vehicle motion model with considering driver behavior decision model, a Kalman Filter (KF) algorithm for predicting vehicle motion/location, and a safety distance threshold model. The simulated experiments and their results are presented in Sections 5 and 6 respectively. Finally, the main conclusions and the future work of this paper are discussed in Section 7.

2. Literature review

This review provides an examination to the research development in the field of Application of VCPS on vehicle crash avoidance system, vehicle motion model and driver behavior decision model, which is subsequently detailed in Sections 2.1, 2.2 and 2.3 respectively.

2.1. Application of VCPS on vehicle crash avoidance system

The main goal of vehicular cyber physical systems (VCPS) is to improve road traffic safety and mobility. Although current crash avoidance systems (e.g., adaptive cruise control (ACC) systems, lane departure warning systems and lane change assistance systems) have been enhancing road safety, many improvements are still required.

Current VCPSs mainly work in three ways to support collision avoidance: vehicular autonomous systems, infrastructure-based systems and cooperative vehicle infrastructure systems.

The vehicular autonomous system uses vehicular on-board units (OBUs) to real time detect the related motion status of surrounding vehicles and provide driver warnings in case of danger (Huang et al., 2010). In-vehicle sensors (e.g., radar, infrared sensor and vision) are the most common equipment used by the vehicular autonomous system to acquire traffic information (Ewald and Willhoeft, 2000; Amditis et al., 2005; Jamson et al., 2008). These systems only provide the information regarding surrounding vehicles and other information, such as vehicle motion/location and road geometry are ignored. Thus, their performance is restricted to sense vehicle gap unilaterally and their accuracy is limited, such as forward collision warning system (Kaempchen et al., 2009), lateral collision warning system (Schubert et al., 2010) and lane departure warning system (Wu et al., 2002).

The infrastructure-based systems detect the vehicle collision risk and provide drivers warning based on sensors and Dedicated Short-Range Communication (DSRC) devices installed along roadside. The information provided by the infrastructure can be transferred to in-vehicle warning devices and warn the driver about danger (Nekoui et al., 2009). However, unlike the previously mentioned vehicular sensor-based VCPS systems, they usually cannot function in real time and therefore their capacity is also limited.

Advanced cooperative vehicle infrastructure system (CVIS) can detect the vehicle motion and road condition by an integration of vehicular autonomous systems and infrastructure-based systems, which can comprehensively collect and provide more information regarding driver, vehicle and road for much enhanced safety applications (Toledo-Moreo et al., 2007). This could increase safety for nearby vehicles by enhancing the level of cooperation among vehicles, the object vehicle can track the surrounding vehicles in order to detect risk and send warnings to driver in case of danger. Wang et al. (2013) improved driving safety in intersections by incorporating driving safety related information through vehicle to infrastructure communication and inter-vehicles communication. There is a growing interest to build vehicular cyber physical system based on CVIS (Ammoun et al., 2006; Tan and Huang, 2006; Sukuvaara and Nurmi, 2009; Milanés et al., 2011).

2.2. Vehicle motion model

VCPSs introduced above are required to accurately track or predict vehicle motion/location. The driving risk is judged mainly according to the relative movements between the objective vehicle and surrounding vehicles/obstacles.

On the one hand, the efficiency and accuracy of the vehicle collision avoidance system can be improved if vehicle motion of next moment can be accurately predicted in advance, and drivers can be alerted in time. Several model-based tracking algorithms have been applied for tracking and prediction of target/vehicle maneuvers. Li and Jilkov (2003) provided a comprehensive review to various mathematical motion/dynamics models proposed for tracking maneuvering targets including two degree and three degree maneuver models as well as the coordinate-uncoupled generic models. These models were employed in numerous applications and often showed satisfactory results (Lou et al., 2005; Petrovskaya and Thrun, 2009). However, in most cases, these motion models used in tracking systems only describe the vehicle motion/location in a Cartesian coordinate system, the road curvature is not taken into account when estimate or predict the relative movement (e.g. vehicle gap) between objective vehicle and surrounding vehicles. It will decrease the estimation or prediction accuracy in curved road.

On the other hand, the current time-to-collision (TTC) or headway time (HT) are main parameters used to assess the vehicle collision risk when compared with the corresponding safety threshold (Ullah et al., 2012; Kostikj et al., 2012). Most of the research effort has been focused on using new sensors (radars, laser scanners, stereo vision, etc.) to estimate the TTC or HT between the tracked vehicle and detected obstacles, also the road curvature is ignored in most cases. Obviously, the traveled distance between two approaching vehicles on curved road is not equal to straight-line distance. Therefore, while the scene has been detected and tracked from the sensorial system on curved road, a complex estimation of the TTC or HT should be proposed, the conventional approach for estimating the TTC or HT can be effective on straight lane conditions.

The challenge for the development of next generation collision avoidance system (CAS) in recent years is the environment recognition and reconstruction around the subject vehicle (Polychronopoulos and Scheunert, 2006; Polychronopoulos et al., 2007), in order to implement vehicle collision avoidance meeting the longitudinal, rear and lateral field.

2.3. Driver behavior decision model (DBDM)

The factors influencing the driving volition are, in general, random and obscure in nature, so driver performance under certain volition is often accompanied by complex cognitive psychological process. In general, driving involved the following four processes: perception, identification, volition and execution (Rendon-Velez et al., 2009). First, driver perceives the running state of the vehicle and surrounding traffic information. Second, she or he identifies possible options, e.g., accelerate/decelerate or change lane. Third, the driver will make a decision and then carry out that decision, which is called “volition”. Driver may operate and control vehicle through the clutch pedal, variable speed device, accelerator pedal, steering and/or braking pedal.

Driver's volition has an important impact on the safety of the vehicle being driven and surrounding vehicles. If the driver's volition changes, accident risk will also be different under the same vehicle state. For example, if the speed of the vehicle under study is 60 km/h and the relative distance from the vehicle ahead is 100 m, the acceleration volition would be considered as dangerous/risky. Conversely, if the driving volition is slow-down, the risk level is low and therefore the action should be considered as not dangerous. From this perspective, it appears that existing methods using relative distance only to judge safety is not comprehensive enough to realistically model real-world safety issues. Although the existing models, such as the CA model, can well simulate vehicle movements, operation rules used in these models must be extended, in order to more accurately represent behavioral process impacting vehicle motion, such as acceleration, deceleration and lane change.

Car following models and lane change models have been the most extensively investigated DBDMs. They have been appeared in the following studies. Kishimoto and Oguri (2008) proposed a method for modeling driving behavior extracted from past movements using AR-HMM (Auto-Regressive Hidden Markov Model). It predicts the probability of operation that driver will take during the next short period. Gunnarsson et al. (2006) proposed a method for studying the connection between different driver plans and corresponding motion models, which enables a formal prediction of the driver volition that would most likely take place. Lidstrom and Larsson (2008) predict future states of traffic environment based on a combination of a fuzzy logic model considering intersection turning behavior and a Gipps model considering car following behavior. Mobus et al. (2003) proposed an optimal acceleration model for a multi-vehicle traffic scene. The “optimal” acceleration/deceleration rate is found by respecting traffic rules, safety distances and driver volitions. In addition, Hamdar et al. (2008) explored a car following model, which explicitly considers the psychological and cognitive aspects of driving decision-making process. Prospect theory is adopted to evaluate and weigh driver's alternatives, including acceleration, deceleration or maintain a constant speed. The authors discuss how the model can be used to capture risk taking behavior under uncertainty. However, none of the driver behavior models presented in the literature has quantitatively considered driver behavior, e.g., accelerate or decelerate with a particular acceleration/deceleration rate at a given time (e.g., $a = 2 \text{ m/s}^2$). Due to such a deficiency, they are not appropriate as a component of a vehicle motion model.

3. Overall architecture of the VCPS-based collision risk assessment system

In this section, the architecture of the proposed VCPS-based collision risk assessment system is shown in Fig. 1, and the corresponding simulation platform is developed based on CARSIM, which will be applied for collision risk assessment in Section 5.

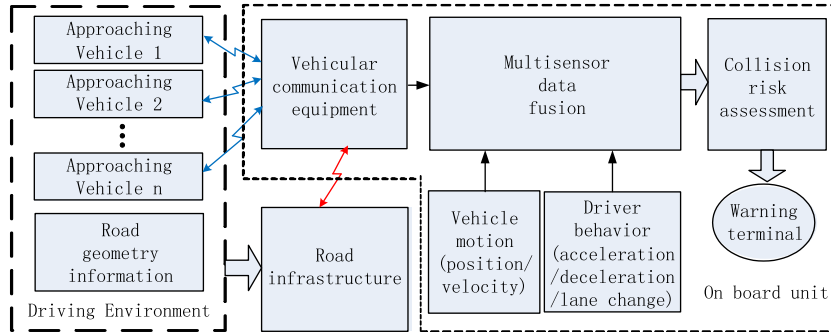


Fig. 1. The architecture of the proposed collision warning system.

The proposed VCPS consists of the following five simulated modules: vehicular sensors, roadside equipment, data fusion, risk assessment and warning device. With vehicular sensors and roadside equipment, safety-related information, such as driver behavior, vehicle motion/location and road curvature, can be comprehensively captured and collected. Then, such information is transferred to and then processed by the data fusion unit, in order to predict vehicle motion/location and estimate the gap among surrounding vehicles. After that, the vehicular safety distance threshold is calculated based on relative vehicle speed and compared with the predicted vehicular gap within the risk assessment unit. Finally, the warning device will promote driver when the estimated vehicular gap is smaller than the calculated vehicular safety distance threshold.

It should be noted that the architecture of the proposed VCPS can be easily implemented in field, because the vehicular sensors and roadside equipment have been widely implemented (Kishimoto and Oguri, 2008; Gunnarsson et al., 2006; Lidstrom and Larsson, 2008).

In this paper, we mainly focus on testing the feasibility of the proposed data fusion and collision risk assessment method through the simulated VCPS. It is also assumed that the road curvature in every simulated point can be acquired by roadside equipment, so does vehicle motion/location by vehicular location system (e.g., Global Position System, Inertial Navigation System). It should be noted that, the virtual roadside equipment and vehicular location system in this paper have been simulated and implemented by the simulation software – Carsim.

4. Methodology

This section presents a traffic information fusion to comprehensively process vehicles' motion on curved road and evaluate the driving safety. The vehicles' driving parameters (e.g. location, speed and acceleration) are estimated and predicted, and the driving situation of each V2V surveyed vehicle is assessed in real time.

4.1. Road description and travel distance estimation

In this section, vehicle motion is first described in Cartesian coordinate system ($\varepsilon_x, \varepsilon_y$) and then transferred into a vehicle-based coordinate system (η_x, η_y), in order to accurately calculate the gap between vehicles (in Fig. 2).

Then, a time discrete vector \mathbf{X}_k is set to describe vehicle motion/location \mathbf{x}_k^i ($i = 1, 2, \dots, n$) and road geometry in terms of curvature r_k^T . The state vector \mathbf{X}_k can be represented as

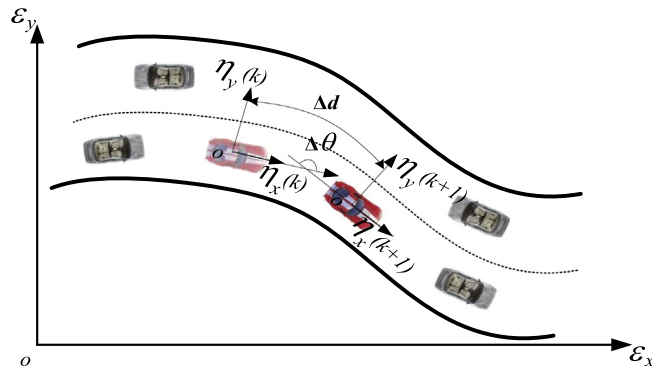


Fig. 2. Cartesian coordinate system and vehicle-based referencing system.

$$\mathbf{X}_k = [(x_k^1)^T (x_k^2)^T \dots (x_k^n)^T r_k^T]^T$$

where x_k^i ($i = 1, 2, \dots, n$) is the motion state vector for the i th vehicle traveling on a road under the surveillance of vehicular cyber physical system, and the vector r_k represents the road parameters. The subscript k is the notation for a k th discrete time point by that time $t = t_k$, the continuous time interval between two samples is a constant T_s , which is denoted as $T_s = t_k - t_{k-1}$.

A set of models are applied in this work to estimate the x_k^i and r_k . A clothoid model, which is similar to what used by Toledo-Moreo et al. (2010) and Sorstedt et al. (2011), is used to describe the road geometry in terms of curvature, which is in the following form:

$$\tau_0(k+1) = \tau_0(k) + \tau_1(k) * \Delta d \quad (1)$$

The parameter $\tau_0(k)$ is the local curvature at the k th vehicle location, and the $\tau_1(k)$ is the corresponding curvature change rate. The coordinate system $(\eta_x(k), \eta_y(k))$ and $(\eta_x(k+1), \eta_y(k+1))$ respectively represent the vehicle's location at time k and $k+1$. Δd is the traveled distance during $[k, k+1]$, which can be described as

$$\Delta d = \frac{\tau_0(k+1) - \tau_0(k)}{\tau_1(k)} \quad (2)$$

Within a vehicular cyber physical system, $\tau_0(k)$ and $\tau_1(k)$ can be easily identified by sensors according to the vehicle's location. Thus, the traveled distance during $[k, k+1]$ can be estimated through Formulas (2).

4.2. Vehicle prediction model

The vehicle motion and its states can be represented accurately by some well-known state-space models, which are usually in the following form:

$$\begin{cases} \mathbf{x}_{k+1} = f(\mathbf{x}_k, \mathbf{u}_k) + \mathbf{w}_k \\ \mathbf{z}_k = h(\mathbf{x}_k) + \mathbf{v}_k \end{cases} \quad (3)$$

where \mathbf{x}_k , \mathbf{z}_k and \mathbf{u}_k are the target state, the observed state, and the control input at the discrete time t_k ; \mathbf{w}_k and \mathbf{v}_k are the process and measurement noise respectively. Function $f()$ is the function of \mathbf{x}_k and \mathbf{u}_k , and $h()$ is the function of \mathbf{x}_k . Such motion models are popular in vehicle tracking applications because they use simple and efficient algorithms such as Kalman Filter (KF) to estimate and predict the vehicle's real state from sensor data.

A frequently used linear motion model is the Constant Acceleration (CA) model, which can be described with state equations, observation equations and initial conditions by the following:

$$\mathbf{Z}_{k+1} = \mathbf{A}_k \mathbf{Z}_k + \mathbf{B}_k \mathbf{w}_k \quad (4)$$

Furthermore, it is assumed that the observation model is set as follow:

$$\mathbf{S}_k = \mathbf{Z}_k + \mathbf{v}_k \quad (5)$$

This motion model enables efficient prediction algorithms such as KF to estimate the future states. The motion status vector \mathbf{Z}_k is defined as

$$\mathbf{Z}_k = [X_k Y_k \dot{X}_k \dot{Y}_k \ddot{X}_k \ddot{Y}_k]^T$$

where (X_k, Y_k) is the position of the vehicle, and (\dot{X}_k, \dot{Y}_k) is the first order derivative of X_k and Y_k , therefore they represent the longitudinal and lateral speed of the vehicle. (\ddot{X}_k, \ddot{Y}_k) is the second order derivative of X_k and Y_k , and they represent the acceleration rates along the longitudinal and lateral direction. \mathbf{S}_k is the observation value. \mathbf{A}_k is the state transition matrix, and \mathbf{B}_k is the control weighting matrix of system input, which take the following form:

$$\mathbf{A}_k = \begin{bmatrix} 1 & 0 & T_s & 0 & \frac{T_s^2}{2} & 0 \\ 0 & 1 & 0 & T_s & \frac{T_s^2}{2} & 0 \\ 0 & 0 & 1 & 0 & T_s & 0 \\ 0 & 0 & 0 & 1 & 0 & T_s \\ 0 & 0 & 0 & 0 & 1 & 0 \\ 0 & 0 & 0 & 0 & 0 & 1 \end{bmatrix}, \quad \mathbf{B}_k = \begin{bmatrix} \frac{T_s^2}{2} & 0 \\ 0 & \frac{T_s^2}{2} \\ T_s & 0 \\ 0 & T_s \\ 1 & 0 \\ 0 & 1 \end{bmatrix}$$

The process noise \mathbf{w}_k is an acceleration change over a period $[t_k, t_{k+1}]$. \mathbf{v}_k represents discrete noise measurements, and it is a vector of an independent process sequence. \mathbf{w}_k and \mathbf{v}_k are white noise, which are zero-mean and independent to each other, and are satisfying the following conditions:

$$\begin{aligned} E[\mathbf{w}_k \mathbf{w}_j^T] &= \mathbf{Q}_k \delta_{kj} \\ E[\mathbf{v}_k \mathbf{v}_j^T] &= \mathbf{R}_k \delta_{kj} \\ E[\mathbf{w}_k \mathbf{w}_j^T] &= 0 \end{aligned}$$

Obviously, the CA model fails to account for the driver's control input, as it doesn't include a term of driver control. Although prediction methods, such as KF, have adaptive mechanisms for eliminating errors caused by model inaccuracy, prediction results are affected by modeling error to some extent. The CA model can be improved if we incorporate the driver control input u_k . The improved CA model is described as below:

$$Z_{k+1} = A_k Z_k + B_k (u_k + w_k) \quad (6)$$

where $u_k = [\Delta a_x \Delta a_y]^T$ is driver's input which represents the error between driver expected vehicle acceleration/deceleration and real acceleration/deceleration. In this way, the driver's input is no longer represented as the white noise. The improved model is found to be more accurate to the real situation.

According to Kalman prediction method (Cheok et al., 2000), the next motion status can be described as follow formulas:
The forecast step:

$$\hat{Z}_{k+1|k} = A_k \hat{Z}_{k|k} + B_k u_k \quad (7)$$

The forecast covariance is:

$$P_{k+1|k} = A_k P_{k|k} A_k^T + B_k Q_k B_k^T \quad (8)$$

The Kalman gain matrix:

$$K_{k+1} = P_{k+1|k} [P_{k+1|k} + R_k]^{-1} \quad (9)$$

The estimation step is:

$$\hat{Z}_{k+1|k+1} = \hat{Z}_{k+1|k} + K_{k+1} [S_{k+1} - \hat{Z}_{k+1|k}] \quad (10)$$

The estimation covariance is:

$$P_{k|k} = [I - K_k] P_{k+1|k} [I - K_k]^T + K_k R_k K_k^T \quad (11)$$

4.3. Optimal driver control input

In this part, the optimal driver control input for the car following scenario are described, as shown in Fig. 3.

When the distance between the subject vehicle and the preceding vehicle is less than a critical value, the preceding vehicle is assumed to impede the subject vehicle. The subject vehicle is required to keep a certain distance from the vehicle ahead by maintaining a similar speed with the preceding vehicle. In this case the vehicle motion is transformed from “free driving” to “following” in the simulation. The equation for describing the motion of above two vehicles can be described as the following:

$$\begin{cases} \dot{D}_l(t) = V_r(t) = V_p(t) - V_{own}(t) \\ \dot{V}_r(t) = a_p(t) - a_{own}(t) \end{cases} \quad (12)$$

where D_l is the gap between the two vehicles, V_r is the relative velocity, V_p is the velocity of the preceding vehicle, V_{own} is the velocity of the subject vehicle, a_p is the acceleration rate of the preceding vehicle, a_{own} is the acceleration rate of the following vehicle. When D_l is far greater than a threshold D_{safe} , driver is assumed to take an operation strategy for free driving where the driver will only take actions necessary to maintain a comfortable driving. D_{safe} is the safe distance threshold between the preceding vehicle and the subject vehicle. Drivers are assumed to maintain a preferred velocity and they are reluctant to frequently change speed. Thus, driver's preferred behavior during period $[t_0, t_f]$ can be described by the cost function as below:

$$J_{\text{preferred}} = \int_{t_0}^{t_f} (a_{own}^T \cdot R \cdot a_{own}) dt \quad (13)$$

where R is the weight of the acceleration a_{own} . In addition, driver feels a significant discomfort when vehicle acceleration goes beyond the scope of -2.5 m/s^2 to 1 m/s^2 (Hou et al., 2005). Thus, the driver's input is viewed as an admissible control:

$$-2.5 < a_{own} < 1$$

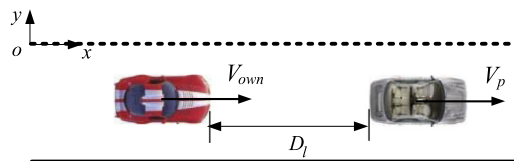


Fig. 3. Car following scenario.

When D_l approximates to D_{safe} , the subject vehicle is forced to transform into the following driving status. When the vehicles are in the “following” status, drivers mainly focus on maintaining a safe distance between their own vehicle and the vehicle ahead. This is achieved by controlling the speed of their vehicle to ensure safety. In order to capture the driver behavior for maintaining a safe distance, the following cost function is developed to reflect the above behavior during period $[t_0, t_f]$. The “safety” cost is calculated as:

$$J_{\text{safety}} = \int_{t_0}^{t_f} (k_1 \cdot \Delta x^2(t) + k_2 \cdot V_r^2(t)) dt \quad (14)$$

where $\Delta x(t) = D_l(t) - D_{safe}$. k_1 and k_2 is the weight of state variables. Then the total cost for the “car following” scenario can be calculated by adding the above two functions together, which can be described as:

$$J_f = J_{\text{safety}} + J_{\text{preferred}} = \int_{t_0}^{t_f} (k_1 \cdot \Delta x^2(t) + k_2 \cdot V_r^2(t) + a_{own}^T \cdot R \cdot a_{own}) dt \quad (15)$$

The model can be used to simulate drivers with different characteristics, who may weigh safety and comfort different, by choosing appropriate weight values (i.e. k_1 , k_2 , R) in the above equation. When the total cost J_f is minimized, the expected acceleration a_{own}^* can be obtained based on the LQR method. The cost function for the car following scenario reflects the driver's desire to maintain a specific speed given by the parameter a_{own}^* , and in this case, the expected lateral acceleration is assumed to be zero. Thus, in this scenario, the driver control input can be described as:

$$u_k = \begin{bmatrix} \Delta a_x \\ \Delta a_y \end{bmatrix} = \begin{bmatrix} a_{own}^* - \ddot{X}_k \\ 0 - \ddot{Y}_k \end{bmatrix}$$

4.4. Collision risk detection

In general, drivers tend to focus on current velocity in order to ensure a safe distance between their own vehicles and the surrounding vehicles, pedestrians and other obstacles ahead. When the distance between the subject vehicle and the preceding vehicle is less than a critical value, the preceding vehicle is assumed to impede the subject vehicle. The subject vehicle is required to keep a certain distance from the vehicle ahead. In this case the vehicle motion is transformed from “free driving” to “following” in the simulation. If the subject vehicle runs in the “following” status, the preceding vehicle imposes certain restriction onto the subject vehicle, then it should be considered a safety distance between the subject vehicle and the preceding vehicle. Else, none of crash accident will occur on the subject vehicle when it runs in the “free driving” status.

The vehicle collision risk is assessed based on safety distance threshold that the objective vehicle and obstacles (only vehicle–vehicle accident case is considered in this section) should keep at least. A suitable braking distance of following vehicle is calculated to represent the safety distance according to Hou et al. (2005), and the common traffic scenario is shown in Fig. 4.

In Fig. 4, D_l denotes distance between subject vehicle and front vehicle, v_p and v_{own} respectively denotes speed of subject vehicle and front vehicle. Then, the threshold of safe distance D_s is calculated as:

$$D_s = \frac{(v_{own} - v_p)^2}{2 * (0.0524 * v_{own} - 0.1215)} + 0.8509 * v_p + 1.6 \quad (16)$$

In essence, the CA model described in formulas (4) is a kinematic particle model, where the vehicle motion is decoupled in different dimensions. In this section, the vehicle speed in the curved road coordinate system can be calculated based on vehicle's head θ and (v_x, v_y) , thus the v_{own} can be described as

$$v_{own} = v_x / \cos \theta \quad (17)$$

Other vehicle's speed can be calculated with the same way.

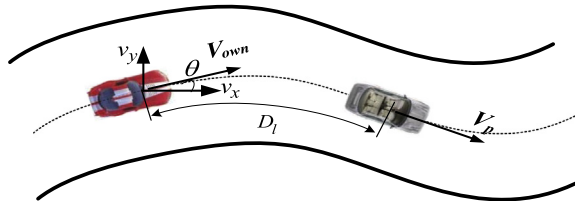


Fig. 4. Traffic driving scenario.

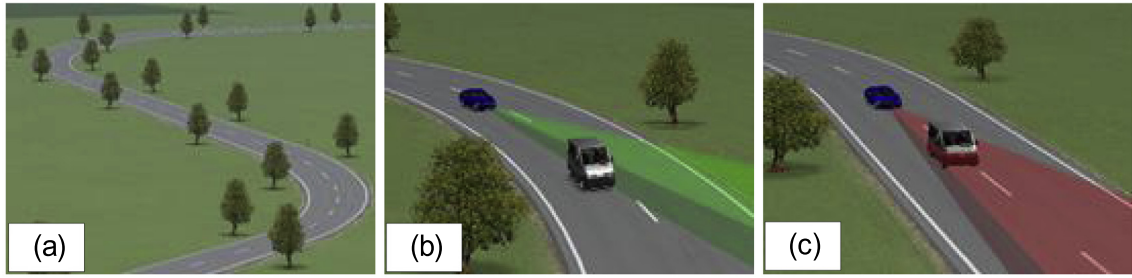


Fig. 5. Simulated test scenarios.

5. Simulation and evaluation

In this section, simulated driving tests are carried out and prediction results of vehicles related motion status from this simulated VCPS are evaluated. The predicted vehicle gap and predicted safe distance threshold are compared to identify the collision risk. The simulation platform is developed based on CARSIM. Simulated driving tests are carried out over a section of curved, one-way, two-lane roadway as shown in Fig. 5(a). Typical traffic parameters are set up to simulate the scenarios that cannot be easily recorded in real-world due to safety concerns. The sections, showing the acceleration, deceleration and keeping lane from the simulation processes of the testing vehicles, are extracted and carefully studied, which are shown in Fig. 5(b) and (c). In order to simplify the analysis, only a sedan in dark blue and a Sports Utility Vehicle (SUV) in white carried on the simulation scenarios. Two vehicles are traveling along the curved road and the dark blue vehicle follows the white vehicle.

In each simulation run, vehicle motions are controlled by a “simulation driver” on the simulated road as shown in Fig. 5. During this simulation process, the blue sedan is placed far away from the preceding white SUV. As the sedan driver feels the distance with the preceding vehicle is too close and it impedes the movement of the sedan, then the simulated driver will decelerate the sedan to ensure a safe distance with the preceding vehicle, as shown in Fig. 5(b). When the blue sedan is simulated to accelerate and then the gap with the preceding vehicle is rapidly reduced, as shown in Fig. 5(c). The initial speed and location of all simulated vehicles are specified. All simulated experiments are repeated under same condition for several times.

The observed data for describing road line and vehicle motion, such as vehicle position, speed and road curvature, are post-processed by adding white noise, in order to make the simulation runs more like the data acquired by sensor in the field. Then, the KF method is applied to predict position and speed of the testing vehicles based on the proposed method in Section 4.2. Monte-Carlo method is used to repeat the simulation and the mean error of prediction is calculated as:

$$\bar{e}_x(k) = \frac{1}{M} \sum_{i=1}^M [x_i(k) - \hat{x}_i(k|k-1)] \quad (18)$$

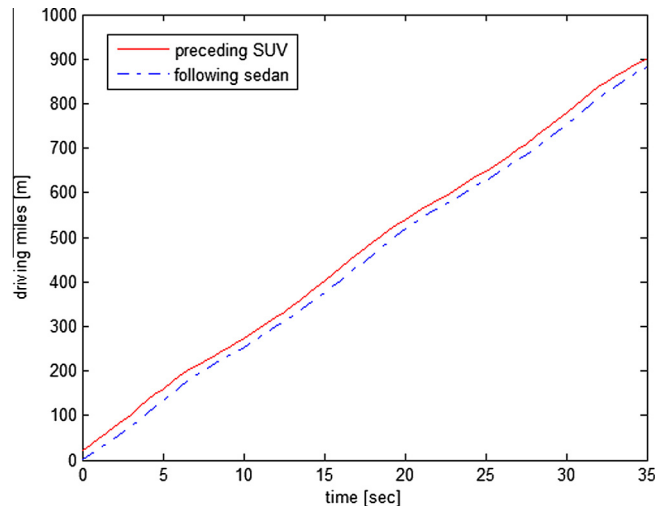


Fig. 6. Traveling distance of the two vehicles in simulation scenario.

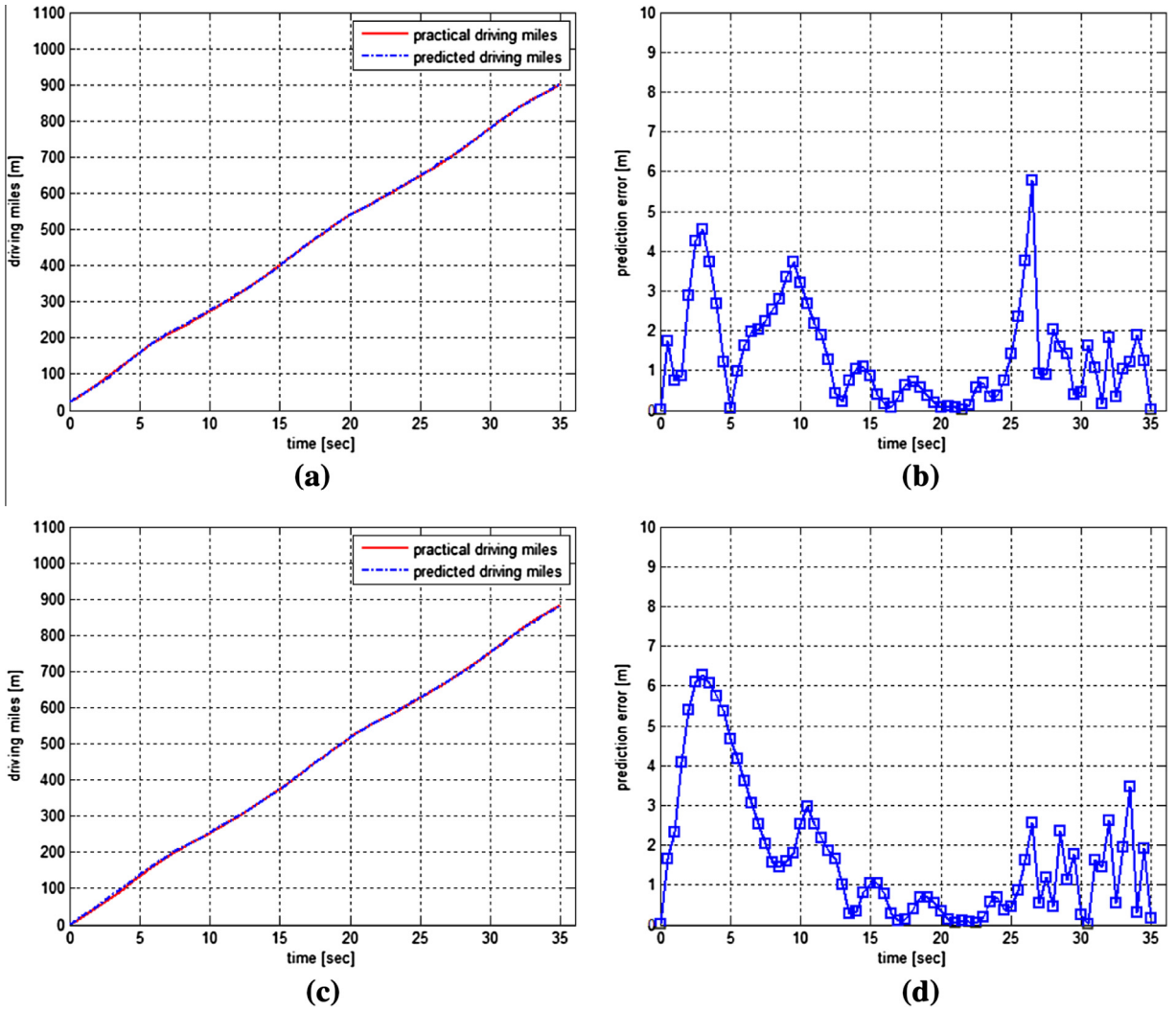


Fig. 7. Driving miles prediction and error.

where M is the number of Monte-Carlo simulations, x_i and \hat{x}_i is the simulated and predicted position, speed and acceleration/deceleration rates of the testing vehicle respectively.

The performance of the collision risk assessment method is evaluated through the receiver operating characteristic (ROC) curve analysis. ROC curve can illustrate the performance of a binary classifier system through comparing two operating characteristics as the criterion changes. It is created by plotting the fraction of true positives out of the total actual positives TPR (true positive rate) vs. the fraction of false positives out of the total actual negatives FPR (false positive rate) (Chambless and Diao, 2006).

In this study, the simulated and predicted vehicle gap and safe distance threshold are calculated according to the method presented in Section 4. The collision risk is assessed by comparing the vehicular gap and the corresponding safe distance threshold, for both the simulated and predicted pairs. In this study, four scenarios are defined as follows: if both the simulated scenario and the predicted situation are judged as dangerous, the assessment result is defined as true positive (TP); if the simulated scenario is judged as safe but the predicted scenario as dangerous, the assessment result is defined as false positive (FP); if the simulated scenario is judged as dangerous but the predicted scenario as safe, the assessment result is defined as false negative (FN); if both the simulated scenario and the predicted situation are judged as safe, the assessment result is defined as true negative (TN). According to inference, the TPR (true positive rate) and FPR (false positive rate) can be represented as,

$$\text{TPR} = \frac{\text{TP}}{\text{TP} + \text{FN}}$$

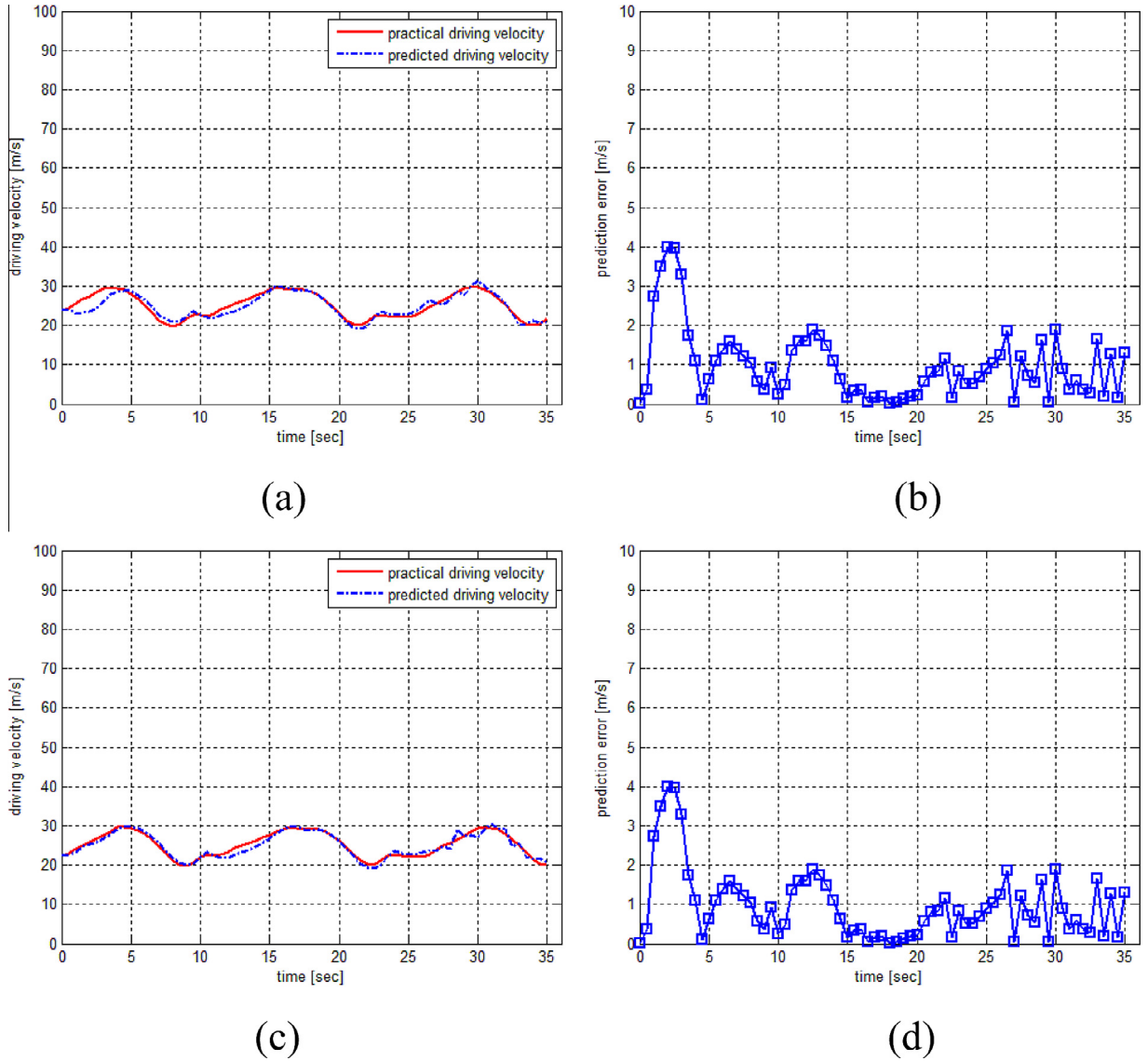


Fig. 8. Speed prediction and error.

$$FPR = \frac{FP}{FP + TN}$$

Then, the ROC curve can be developed by plotting the fraction of true positives (TPR = true positive rate) versus the fraction of false positives (FPR = false positive rate). The area under the ROC curve (AUC) can then be used to assess the overall identification accuracy of the proposed method.

6. Results and discussion

In this section, the power of vehicles motion prediction and the performance of driving situation assessment based on proposed method are evaluated by comparing the prediction errors of vehicle motion regarding future driving status. The traveled distance of the white SUV (preceding vehicle) and the blue sedan (following vehicle) in simulation test is shown in Fig. 6.

The prediction results of the traveled distance of preceding vehicle and following vehicle are plotted in Fig. 7(a) and (c), and their prediction errors are plotted in Fig. 7(b) and (d).

In Fig. 7(a) and (c), the red solid lines represent the true vehicle traveled distance, the blue dotted lines represent the corresponding predicted parameters from the vehicle motion model. The high similarity between the solid line and dotted line in these plots show good performance in vehicle travel path prediction.

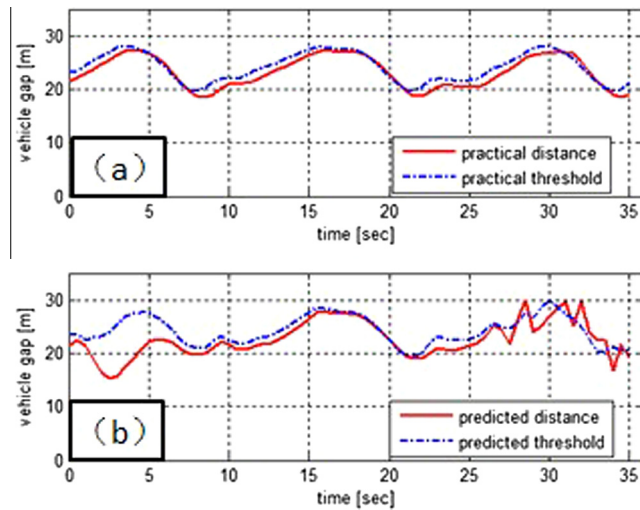


Fig. 9. Practical and predicted vehicle gap.

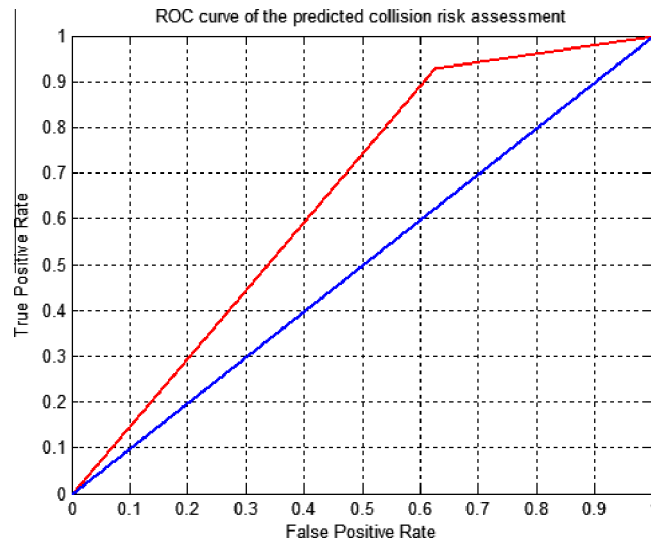


Fig. 10. ROC curve of predicted driving risk identification.

The accuracy of the travel path estimation is studied by calculating mean error (ME) related to the traveled distance of the testing vehicles. The corresponding ME is plotted in Fig. 7(b) and (d) respectively. It can be seen that the prediction error become higher at beginning and some outliers, for examples, at $t = 27$ s, the predicted traveled distance of preceding vehicle is about 6 m, which is higher than at other times. However, the prediction results are very close to the real vehicle travel path at most of time. The accurate prediction from the proposed method can be served for developing a practical driver assistance system.

The driving speed of preceding vehicle and following vehicle are plotted in Fig. 8(a) and (c) respectively, and their prediction errors are plotted in Fig. 8(b) and (d). It can also be seen that the real travel speed and the predicted results are very close.

MEs are used to evaluate the estimation accuracy of the testing vehicles' speed. The corresponding ME is plotted in Fig. 8(b) and (d) respectively. They indicate that the speedy prediction errors keep in a small range after beginning time. The above results confirm that the speed prediction of proposed method is feasible and accurate to estimate vehicle safe distance threshold according to formulas (16).

It is clear from the above results that the proposed method is found to significantly perform well in predicting vehicle's location and speed.

The future state of each vehicle is estimated based on a Kalman Filter (KF) prediction method. The motion status of each vehicle can be communicated with other surrounding vehicles by vehicular cyber systems (e.g. V2V, V2I), then, both the

simulated and predicted vehicular gap can be estimated. The simulated vehicular distance and safe distance threshold between blue sedan and preceding SUV are shown in Fig. 9(a), and the corresponding predicted vehicle gap and safe distance threshold are shown in Fig. 9(b).

If the simulated vehicle gap is shorter than the corresponding safe distance threshold, as shown in Fig. 9(a), at $t = 2$ s, the proposed collision avoidance system will alarm driver for a brake action to avoid the collision. Similarly, the predicted vehicle gap and safe distance threshold are also estimated and compared, as shown in Fig. 9(b). At $t = 4$ s, the predicted vehicle gap is shorter than the safe distance threshold (SDT), which has same results as the simulated scenario at $t = 4$ s. Since the two scenarios reach a same assessment result, it supports that the prediction result is correct. On the contrary, at $t = 28$ s, the simulated vehicle gap is shorter than the corresponding SDT, while the predicted vehicle gap is longer than the predicted SDT, and therefore it can be concluded that the prediction result is incorrect.

The accuracy of the proposed collision risk assessment method is further evaluated based on an ROC curve analysis, as shown in Fig. 10. The false positive rate is 0.9273, while the true positive rate is 0.625. The area under the ROC curve is 0.6512, which is well beyond 0.5 and therefore confirms the effectiveness of the proposed collision risk assessment method.

7. Conclusions

It is clear from the above results that the improved model is found to significantly outperform the CA model in predicting vehicle's position, velocity and acceleration/deceleration. The study results clearly suggest that driver behavior should be considered when tracking/predicting vehicle motion.

Literature review indicates that previous CASs fall short in using predicted vehicle motion/location and road geometry (e.g., curvature) for risk assessment. In this paper, a collision risk assessment method based on a simulated vehicular cyber-physical system is presented. Basically, it considers more safety-related information, such as driver behavior, predicted vehicle motion/location and curved road geometry, than previous CASs. Collision risk can be estimated through predicting the motion and location of each vehicle in real time. Statistical analysis shows that the MEs of vehicle location prediction are mostly less than 4 m and those of vehicle speed prediction are mostly smaller than 2 m/s. In addition, the ROC curve analysis shows that the Area under the Curve of the ROC (AUC) is greater than 0.5. It is believed that the proposed system should be effective for detecting crash risk and providing accurate warnings in a prompt manner.

Future work shall involve modifying the existing vehicle motion prediction model to better capture driver behavior, like lane changing and overtaking, as a control input to improve the prediction performance of the proposed system. Another challenge is to design a suitable driver model as an add-on of the system presented here, in order to reflect different driving styles during complex vehicle maneuvers, such as overtaking and U-turn. Lastly, the proposed system should be tested in a real-world VCPs test-bed.

Acknowledgments

The study is supported by the National Nature Science Foundation of China (Nos. 51178364, 61104158, 51105286), the Excellent Youth Foundation of Hubei Scientific Committee (2012FFA023) and the Discipline leader program of Wuhan Science and Technology bureau (201271130445).

References

- Amditis, A., Polychronopoulos, A., Floudas, N., Andreone, L., 2005. Fusion of infrared vision and radar for estimating the lateral dynamics of obstacles. *Inf. Fusion* 6 (2), 129–141.
- Ammoun, S., Nashashibi, F., Laugeau, C., 2006. Real-time crash avoidance system on crossroads based on 802.11 devices and GPS receivers. In: *IEEE Intelligent Transportation Systems Conference*, pp. 1023–1028.
- Chambless, L.E., Diao, G., 2006. Estimation of time-dependent area under the ROC curve for long-term risk prediction. *Stat. Med.* 25 (20), 3474–3486.
- Cheok, K.C., Smid, G.E., McCune, D.J., 2000. A multisensor-based collision avoidance system with application to a military HMMWV. In: *Proceedings of Intelligent Transportation Systems*, pp. 288–292.
- Ewald, A., Willhoeft, V., 2000. Laser scanners for obstacle detection in automotive applications. In: *Proc. The IEEE Intelligent Vehicle Symposium*, pp. 682–687.
- Gunnarsson, J., Svensson, L., Bengtsson, F., Danielsson, L., 2006. Joint driver volition classification and tracking of vehicles. In: *Proc. Nonlinear Stat. Signal Process. Workshop*, pp. 95–98.
- Hamdar, S.H., Treiber, M., Mahmassani, H.S., Kesting, A., 2008. Modeling driver behavior as sequential risk-taking task. In: *87th Meeting of the Transportation Research Board*, pp. 208–217.
- Huang, W., Rong, H., He, J., Gong, J.F., 2010. Design and implementation of distributed large vehicle collision warning system. *J. Transp. Inf. Saf.* 28 (4), 81–85.
- Jamson, A.H., Lai, F.C.H., Carsten, O.M.J., 2008. Potential benefits of an adaptive forward collision warning system. *Transp. Res. Part C Emerg. Technol.* 16 (4), 471–484.
- Kaempchen, N., Schiele, B., Dietmayer, K., 2009. Situation assessment of an autonomous emergency brake for arbitrary vehicle-to-vehicle collision scenarios. *IEEE Trans. ITS* 10 (4), 678–687.
- Kishimoto, Y., Oguri, K., 2008. A modeling method for predicting driving behavior concerning with driver's past movement. In: *IEEE International Conference on Vehicular Electronics and Safety*, Columbus, pp. 132–136.
- Kostikj, A., Kjosovski, M., Kocarev, L., 2012. Harmonized traffic stream in urban environment based on adaptive Stop&Go cruise control and its impact on traffic flow. In: *IEEE International Conference on Vehicular Electronics and Safety*, pp. 140–145.
- Liu, Z.Q., Wang, P., Qin, H.M., et al., 2010. Study on intelligent anti-collision for warning technology based on multi-information detection. *China Saf. Sci. J.* 20 (1), 153–158.
- Li, X.R., Jilkov, V.P., 2003. Survey of maneuvering target tracking. Part I: Dynamic models. *IEEE Trans. Aerosp. Electron. Syst.* 39 (4), 1333–1364.

- Lidstrom, K., Larsson, T., 2008. Model-based estimation of driver volitions using particle filter. In: IEEE Int. Conf. Intelligent Transportation Systems, pp. 1177–1182.
- Lou, J., Tan, T., Hu, W., Yang, H., Maybank, S., 2005. 3-D model-based vehicle tracking. *IEEE Trans. Image Process.* 14 (10), 1561–1569.
- Hou, D.Z., Liu, G., Gao, F., Li, K.Q., Lian, X.M., 2005. A new safety distance model for vehicle collision avoidance. *Automot. Eng.* 27 (2), 186–190.
- Milanés, V., Alonso, J., Bouraoui, L., Ploeg, J., 2011. Cooperative maneuvering in close environments among cybercars and dual-mode cars. *IEEE Trans. Intell. Transp. Syst.* 12 (1), 15–24.
- Mobus, R., Baotic, M., Morari, M., 2003. Multi-object adaptive cruise control. In: Proc. Int. Conf. Hybrid Systems: Computation and Control, pp. 359–374.
- Nekoui, M., Daiheng, N., Pishro-Nik, H., Prasad, R., Kanjee, M.R., Hui, Z., Thai, N., 2009. Development of a VII-enabled prototype intersection collision warning system. In: Proc. Int. Conf. Testbeds and Res. Infrastructure for Development of Networks & Communities, pp. 1–8.
- Petrovskaya, A., Thrun, S., 2009. Model based vehicle detection and tracking for autonomous urban driving. *Auton. Robots* 26, 123–139.
- Polychronopoulos, A., Scheunert, U., 2006. Revisiting the JDL model for automotive safety applications: the PF2 functional model. In: Proceedings of Information Fusion, pp. 1–7.
- Polychronopoulos, A., Tsogas, M., Amditis, A.J., Andreone, L., 2007. Sensor fusion for predicting vehicles' path for collision avoidance systems. *IEEE Trans. Intell. Transp. Syst.* 8 (3), 549–562.
- Rendon-Velez, E., Horváth, I., Opiyo, E.Z., 2009. Progress with situation assessment and risk prediction in advanced driver assistance systems: A survey. In: Proceedings of the 16th ITS World Congress, pp. 21–25.
- Schubert, R., Schulze, K., Wanielik, G., 2010. Situation assessment for automatic lane-change maneuvers. *IEEE Trans. ITS* 11 (3), 607–616.
- Sorstedt, J., Svensson, L., Sandblom, F., Hammarstrand, L., 2011. A New Vehicle Motion Model for Improved Predictions and Situation Assessment. *IEEE Trans. ITS* 12 (4), 1209–1219.
- Sukuvaara, T., Nurmi, P., 2009. Wireless traffic service platform for combined vehicle-to-vehicle and vehicle-to-infrastructure communications. *IEEE Wirel. Commun.* 16 (6), 54–61.
- Tan, H., Huang, J., 2006. DGPS-based vehicle-to-vehicle cooperative collision warning: engineering feasibility viewpoints. *IEEE Trans. Intell. Transp. Syst.* 7 (4), 415–428.
- Toledo-Moreo, R., Zamora-Izquierdo, M.A., Ubeda-Miarro, B., Gomez-Skarmeta, A.F., 2007. High-integrity IMM-EKF-based road vehicle navigation with lowcost GPS/SBAS/INS. *IEEE Trans. Intell. Transp. Syst.* 8 (3), 491–511.
- Toledo-Moreo, R., Zamora-Izquierdo, M.A., 2010. Collision avoidance support in roads with lateral and longitudinal maneuver prediction by fusing GPS/IMU and digital maps. *Transp. Res. Part C Emerg. Technol.* 18 (4), 611–625.
- Ullah, I., Ullah, Q., Ullah, F., Shin, S.Y., 2012. Integrated collision avoidance and tracking system for mobile robot. In: International Conference on Robotics and Artificial Intelligence, pp. 68–74.
- Wang, J.Q., Wang, H.P., Liu, J.X., Li, K.Q., 2013. Intersection vehicle driving assistance system based on vehicle to infrastructure communication. *China J. Highway Transp.* 26 (4), 169–175.
- Wu, C.Z., Wang, C.Y., Yang, L.B., 2002. Research on fuzzy control of lateral control in intelligent highway system. *J. Highway Transp. Res. Dev.* 19 (2), 131–133, 137.